Diabetes, Obesity and Metabolism

WILEY

ORIGINAL ARTICLE OPEN ACCESS

Identification of Common Blood Metabolic Derangements Using Magnetic Resonance Signatures of the Pancreas and Liver

Wandia Kimita[1] | Juyeon Ko[2] | Loren Skudder-Hill[3] | Xiatiguli Shamaitijiang[1] | Yutong Liu[1] | Maxim S. Petrov[1]

[1]School of Medicine, University of Auckland, Auckland, New Zealand | [2]College of Medicine, Yonsei University, Seoul, Republic of Korea | [3]Yong Loo Lin School of Medicine, National University of Singapore, Singapore, Singapore

Correspondence: Maxim S. Petrov (max.petrov@gmail.com)

Received: 12 November 2025 | **Revised:** 11 February 2026 | **Accepted:** 16 February 2026

Keywords: diabetes | dyslipidaemia | insulin traits | intra-pancreatic fat deposition | liver | magnetic resonance | pancreas

ABSTRACT

Aim: To investigate whether common disturbances of glucose and lipid metabolism can be automatically identified from magnetic resonance signatures of the pancreas and liver.

Methods: In this proof-of-principle study, 100 individuals with a history of pancreatitis—a relatively homogeneous population at risk for metabolic derangements—underwent magnetic resonance assessment on the same 3.0 Tesla scanner. Automated measurements of fat fraction and water proton transverse relaxation time (R2 water) in the pancreas and liver were obtained. Fasting blood samples were analysed for high-density lipoprotein (HDL) cholesterol, low-density lipoprotein (LDL) cholesterol, triglycerides, glucose and insulin. Associations between magnetic resonance signatures and blood metabolic measures were assessed using generalised additive models adjusted for age, sex and body mass index.

Results: In fully adjusted models, HDL dyslipidaemia was significantly associated with intra-pancreatic fat ($p = 0.015$) and intra-hepatic fat ($p = 0.047$), LDL dyslipidaemia with pancreas R2 water ($p = 0.009$), and triglyceride dyslipidaemia with intra-hepatic fat ($p = 0.046$). Lower HOMA-β was significantly associated with intra-pancreatic fat ($p = 0.001$), intra-hepatic fat ($p = 0.004$), pancreas R2 water ($p = 0.031$) and liver R2 water ($p = 0.014$). Higher HOMA-IR was significantly associated with pancreas R2 water ($p = 0.016$).

Conclusions: Automated magnetic resonance signatures of pancreatic and hepatic tissue composition were significantly associated with clinically relevant disturbances in lipid metabolism and indices of glucose homeostasis. These findings support the feasibility of opportunistic, automated detection of abnormal blood metabolic parameters using high-resolution cross-sectional imaging.

1 | Introduction

The global burden of derangements in glucose and lipid metabolism, such as diabetes, prediabetes and dyslipidaemias, has increased substantially over the past decades [1, 2]. Abnormal glucose and lipid metabolism often underlies several highly prevalent diseases, including cardiovascular diseases and non-alcoholic fatty liver disease [3, 4]. The pancreas and liver–both developed from the embryonic endoderm–regulate glucose and lipid metabolism through intricate inter-organ cross-talks [5–7]. Disruption of these inter-organ pathways can drive a spectrum of metabolic phenotypes, ranging from isolated dyslipidaemia to insulin resistance and overt type 2 diabetes. Mechanistically, hepatic insulin resistance promotes increased hepatic gluconeogenesis and de novo lipogenesis, leading to hyperglycaemia and hypertriglyceridaemia, whereas altered hepatic lipid handling

contributes to ectopic fat accumulation and inflammatory signalling that further impairs insulin action [1, 2]. Conversely, pancreatic β-cell dysfunction and reduced insulin secretion exacerbate hepatic glucose production and alter lipid partitioning, reinforcing a maladaptive cycle between glucose intolerance and dyslipidaemia [2, 5]. In line with these mechanisms, hepatic steatosis is strongly associated with type 2 diabetes, insulin resistance, insulin deficiency and dyslipidaemias, and type 2 diabetes independently predicts progression from steatosis to non-alcoholic steatohepatitis and cirrhosis [8, 9]. Excessive intra-pancreatic fat deposition has likewise been linked to increased risk of diabetes mellitus [6, 10, 11]. Beyond fat, abnormal tissue iron deposition in the liver and pancreas has also been associated with increased risk of metabolic derangements [12, 13].

Modern high-resolution imaging enables comprehensive, non-invasive characterisation of the pancreas and liver, and quantitative imaging biomarkers are increasingly being evaluated as tools for risk stratification and treatment monitoring [14]. Quantitative magnetic resonance provides biophysical parametric measurements, enabling mapping of pancreatic and hepatic tissue properties even in the absence of visually apparent pathology [15]. Recent studies have begun to explore associations between quantitative abdominal magnetic resonance biomarkers and metabolic outcomes such as glycaemic status, insulin resistance and dyslipidaemia [16, 17]. These reports suggest that magnetic resonance-derived measures of ectopic fat and iron are related to metabolic risk and may complement laboratory testing. Compared with traditional blood tests that provide systemic, time-varying snapshots of metabolic state, magnetic resonance-derived signatures offer the potential to quantify organ-specific morphology and tissue composition (e.g., fat and iron content) that may reflect longer-term pathophysiology, support phenotyping and provide mechanistic context for abnormal laboratory results. In addition, once standardised acquisition and automated post-processing are in place, magnetic resonance biomarkers could be generated with reduced operator dependence, improved reproducibility and scalability across large cohorts.

However, despite the widespread availability of magnetic resonance scanners across healthcare settings, few studies have assessed whether recent advances in quantitative imaging and automated analysis can be translated into accurate identification of common derangements of glucose and lipid metabolism [18]. Previous approaches have often been labour-intensive—requiring manual post-processing with an increased risk of measurement error—time-consuming and therefore costly, and/or poorly standardised, limiting their generalisability. To our knowledge, the performance of fully automated, high-throughput, standardised quantitative magnetic resonance assessment of both the pancreas and liver for identifying abnormalities in blood glucose and lipid profiles has not been evaluated. If validated across sites and populations, such approaches could enable opportunistic metabolic risk assessment from routine imaging, facilitate earlier identification of at-risk individuals and support personalised prevention and monitoring strategies.

The present study aimed to investigate whether common metabolic derangements—including diabetes/prediabetes, insulin resistance, insulin deficiency, triglyceride dyslipidaemia, high-density lipoprotein (HDL) dyslipidaemia and low-density lipoprotein (LDL) dyslipidaemia—can be automatically identified from standardised quantitative magnetic resonance signatures of the pancreas and liver.

2 | Methods

2.1 | Study Design and Participants

This cross-sectional study was conducted as part of the COSMOS programme and approved by the New Zealand Health and Disability Ethics Committee (13/STH/182). Adults aged 18 years or older with a history of acute or chronic pancreatitis were eligible to participate, representing a relatively homogeneous population at high risk for new-onset disturbances in glucose and lipid metabolism. Participants were included no earlier than 3 months after clinical resolution of their pancreatitis episode. Exclusion criteria were: pancreatic lipomatosis or lipomatous pseudohypertrophy, pancreatic cysts, hereditary pancreatitis, autoimmune pancreatitis, cystic fibrosis, pancreatic trauma, congenital pancreatic anomalies, post-endoscopic retrograde cholangiopancreatography pancreatitis, intra-operative diagnosis of pancreatitis, any prior pancreatic interventions (surgical, endoscopic or radiologic), ascites, severe chronic obstructive pulmonary disease limiting breath-holding, systemic steroid therapy, malignancy, implanted metallic or electronic devices, cognitive impairment or pregnancy. All participants provided written informed consent prior to enrollment.

2.2 | Magnetic Resonance Signatures

All participants underwent abdominal imaging at the Centre for Advanced Magnetic Resonance Imaging (CAMRI) at the University of Auckland, New Zealand, specifically for the COSMOS programme, using a 3.0 Tesla MAGNETOM Skyra scanner VE 11A (Siemens Healthineers, Erlangen, Germany). The high-speed T2-corrected multi-echo (HISTO) magnetic resonance spectroscopy sequence was employed using a single voxel during a single breath-hold. This sequence, part of the standard commercial product LiverLab (Siemens Healthineers), is designed for quantitative assessment of fat fraction and transverse relaxation time of water protons (R2 water) in target tissues.

Data were acquired from voxels in the liver and in the pancreas, positioned by an experienced medical imaging technologist. Following automated shimming, stimulated echo acquisition mode proton spectroscopy was performed with a repetition time of 3000 ms to minimise T1 weighting. Five spectra were collected at spin-echo times of 12, 24, 36, 48 and 72 ms during a single breath-hold without water suppression. Sequence parameters were: true-form abdomen shim mode, flip angle 90°, water saturation bandwidth 50 Hz, acquisition bandwidth 1200 Hz, acquisition duration 853 ms, 2D spatial mapping, and a 430 mm field of view.

Magnetic resonance spectroscopy data were processed inline using the AI-enabled Siemens Syngo software (Siemens Healthineers) by integrating the water and lipid components

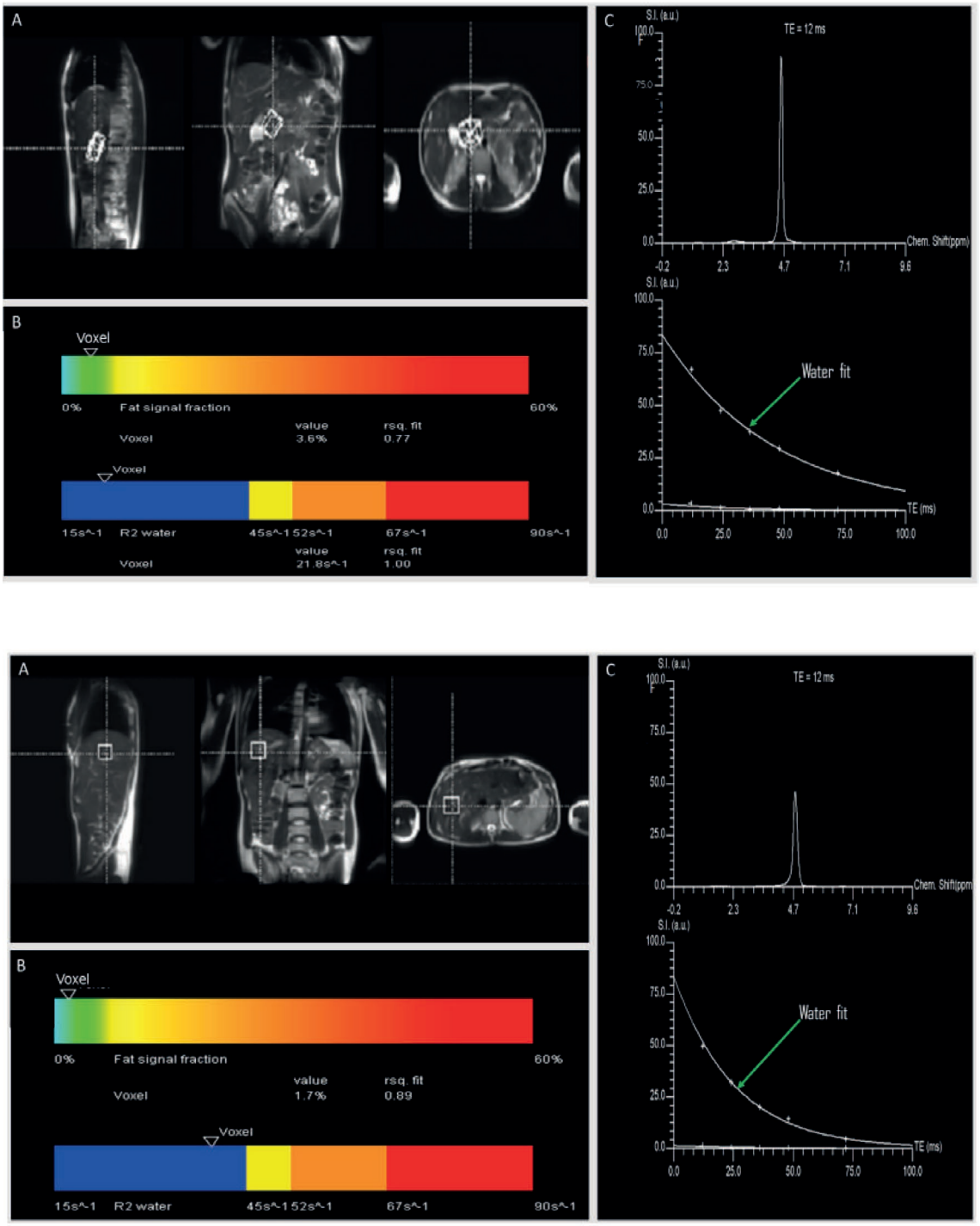

FIGURE 1 | Measurement of fat signal and R2 water using the T2-corrected multi-echo single-voxel (HISTO) sequence. Pancreas (upper panel) and liver (lower panel) fat signal and R2 water acquired in a 66-year-old woman. (A) Voxel location within the tissue. (B) Colour bars depicting fat signal and R2 water values within the single voxel for the entire tissue volume. (C) Fat and water spectra at T2 = 12 ms and the T2 decay curve of water, used to estimate the equilibrium signal.

of each spectrum with T2-relaxation correction. The post-processing output included a T2-corrected spectrum and a table reporting quantitative measures (fat fraction %, R2 water [s^{-1}], and fit error) (Figure 1). Data were exported as DICOM files and viewed using MicroDicom DICOM Viewer (MicroDicom Ltd., Bulgaria). Reporting of this study adhered to the Minimum Reporting Standards for in vivo Magnetic Resonance Spectroscopy [19].

2.3 | Metabolic Assessments

Fasting venous blood samples (≥ 8 h overnight) were collected at the time of the CAMRI visit for analysis of glucose and lipid metabolism biomarkers at the tertiary referral medical laboratory of Auckland City Hospital. Glucose was measured using an enzymatic colourimetric assay (F. Hoffmann-La Roche Ltd., Basel, Switzerland), insulin using a chemiluminescence sandwich

immunoassay (Roche Diagnostic, Auckland, New Zealand), and glycated haemoglobin using a boronate affinity chromatography assay (Trinity Biotech, Wickow, Ireland) on fresh, never-frozen blood.

The lipid panel included high-density lipoprotein (HDL) cholesterol, triglycerides, and total cholesterol, with low-density lipoprotein (LDL) cholesterol calculated using the Sampson formula [20]. The Sampson equation was used because it provides more accurate estimates of LDL cholesterol than older equations, particularly in individuals with elevated triglyceride levels [20]. Homeostasis model assessment of insulin resistance (HOMA-IR) and homeostasis model assessment of pancreatic beta cell function (HOMA-β) were calculated using the HOMA2 calculator (version 2.2.3 Diabetes Trails Unit, University of Oxford, Oxford, UK). Anthropometric measurements (weight, height, waist circumference) and demographic data (age, sex) were obtained by trained personnel using standardised techniques at the time of the CAMRI visit [21].

Metabolic outcomes were derived as binary variables from the above continuous measures. Individuals with glycated haemoglobin ≥ 39 mmol/L were classified as having prediabetes/diabetes [22]. Insulin resistance was defined arbitrarily as HOMA-IR above the cohort median (1.4), and insulin deficiency as HOMA-β below the cohort median (86.4). These cut-off points were used as operational, study-specific groupings to facilitate comparisons (e.g., lower HOMA-β vs. higher HOMA-β) and should not be interpreted as established clinical categories or as implying clinical diagnoses. Triglyceride dyslipidaemia was defined as triglycerides ≥ 1.7 mmol/L, HDL cholesterol dyslipidaemia as HDL ≤ 1.2 mmol/L, and LDL cholesterol dyslipidaemia as LDL ≥ 3.4 mmol/L [23].

2.4 | Statistical Analysis

Analyses were performed using R statistical software (version 4) with the packages mgcv, CatPredi and ggplot2, as well as SAS for Windows (version 9.4; SAS Institute, Cary, NC). Two-tailed *p*-values of less than 0.05 were considered statistically significant. Continuous variables were presented as median (interquartile range, IQR), and categorical variables as counts and percentages.

Data analyses were conducted in two steps. First, associations between four magnetic resonance signatures (log-transformed) and six measures of glucose and lipid metabolism were explored using generalised additive models with P-spline smoothers, both univariable and multivariable (adjusted for age, sex and body mass index). Generalised additive models were chosen for their ability to detect non-linear relationships that linear models may miss. Associations were visualised as partial dependence plots.

Second, the optimal cut-off values for dichotomising continuous imaging biomarkers in multivariable logistic regression models were determined using the R package CatPredi [24]. This method identifies cut-off points that maximise the discriminative ability of the model, measured by the area under the receiver operating characteristic curve (AUC), whereas accounting for non-linear relationships of predictive variables (the four magnetic resonance signatures) with the dependent variable (the six metabolic outcomes) in a logit model. Analyses were adjusted for age, sex and body mass index.

3 | Results

3.1 | Participant Characteristics

A total of 100 adults (35 women) with a median (IQR) age of 59 (48–66) years were included. Other characteristics of the study participants are summarised in Table 1.

3.2 | Identification of Blood Glucose Derangements

HOMA-β was significantly associated with intra-pancreatic fat in the adjusted model only ($p = 0.025$). HOMA-IR was significantly associated with intra-pancreatic fat in the unadjusted model only ($p = 0.037$) and with pancreas R2 water in both the unadjusted ($p = 0.033$) and adjusted ($p = 0.048$) models (Table 2). Glycated haemoglobin showed no significant associations with any imaging biomarkers. These non-linear relationships are illustrated in Figure 2.

TABLE 1 | Characteristics of participants.

Characteristic	*n* = 100
Age (year)	59 (48–66)
Sex	
Men	65 (65%)
Women	35 (35%)
Body mass index (kg/m^2)	27.2 (24.7–32.7)
Intra-hepatic fat (%)	6.7 (3.8–12.5)
Intra-pancreatic fat (%)	20.5 (10.6–29.1)
Liver R2 water (sec-1)	38.3 (35.4–41.8)
Pancreas R2 water (sec-1)	23.0 (21.5–24.6)
Fasting plasma glucose (mmol/L)	5.4 (5.1–6.5)
Fasting insulin (mU/L)	12.1 (7.3–18.5)
Glycated haemoglobin (mmol/mol)	39 (36–46)
HOMA-β	86.3 (67.1–120.3)
HOMA-IR	1.4 (0.9–2.2)
Triglyceride (mmol/L)	1.4 (1.0–2.1)
High-density lipoprotein cholesterol (mmol/L)	1.3 (1.0–1.6)
Low-density lipoprotein cholesterol (mmol/L)	2.8 (2.0–3.5)
Total cholesterol (mmol/L)	4.6 (3.9–5.5)

Note: Data are median (interquartile range) or count (percent).
Abbreviations: HOMA-β, Homeostasis model assessment of β-cell function; HOMA-IR, Homeostasis model assessment of insulin resistance.

TABLE 2 | Associations of glucose and lipid metabolism parameters with magnetic resonance signatures.

	Intra-hepatic fat		Intra-pancreatic fat		Liver R2 water		Pancreas R2 water	
Parameter	**Unadjusted**	**Adjusted**	**Unadjusted**	**Adjusted**	**Unadjusted**	**Adjusted**	**Unadjusted**	**Adjusted**
Glycated haemoglobin	0.092	0.419	0.430	0.578	0.585	0.924	0.112	0.052
HOMA-IR	0.193	0.641	0.037*	0.248	0.600	0.316	0.033*	0.048*
HOMA-β	0.521	0.442	0.052	0.025*	0.811	0.878	0.667	0.319
Triglyceride	0.021*	0.046*	0.671	0.837	0.182	0.199	0.241	0.495
LDL cholesterol	0.746	0.725	0.935	0.681	0.482	0.565	0.031*	0.027*
HDL cholesterol	0.040*	0.301	0.293	0.346	0.435	0.654	0.065	0.666

Note: Data are *p* values for generalised additive models for the relationship between the magnetic resonance signatures as independent variables and glucose and lipid metabolic parameters as dependent variables in univariate and multivariate (adjusted for age, sex and body mass index) models.
Abbreviations: HDL, high-density lipoprotein cholesterol; HOMA-β, Homeostasis model assessment of β-cell function; HOMA-IR, Homeostasis model assessment of insulin resistance; LDL, low-density lipoprotein cholesterol.
*Indicates $p < 0.05$.

Insulin deficiency (lower HOMA-β) was significantly associated with intra-hepatic fat in both the unadjusted ($p = 0.003$) and adjusted models ($p = 0.004$), intra-pancreatic fat in both the unadjusted ($p = 0.003$) and adjusted models ($p = 0.001$), liver R2 water in both the unadjusted ($p = 0.017$) and adjusted models ($p = 0.014$), and pancreas R2 water in the adjusted model only ($p = 0.031$) (Table 3, Figure 3). Insulin resistance (higher HOMA-IR) was significantly associated with pancreas R2 water in both the unadjusted ($p = 0.012$) and adjusted models ($p = 0.016$), as well as with intra-hepatic fat ($p = 0.017$) and intra-pancreatic fat ($p = 0.026$) in the unadjusted model only (Table 3, Figure 3).

Prediabetes/diabetes was significantly associated with intra-pancreatic fat in the unadjusted model ($p = 0.037$), but this association was not observed after adjustment. No significant associations were observed between prediabetes/diabetes and other imaging biomarkers (Table 3, Figure 3).

In summary, HOMA-β was associated with intra-pancreatic fat only after adjustment, whereas HOMA-IR was associated with intra-pancreatic fat only unadjusted but remained associated with pancreas R2 water in both unadjusted and adjusted models; HbA1c showed no significant associations. Lower HOMA-β showed consistent associations with intra-hepatic/intra-pancreatic fat and liver R2 water (and pancreas R2 water only adjusted), whereas higher HOMA-IR was consistently linked only to pancreas R2 water, and prediabetes/diabetes lost its intra-pancreatic fat association after adjustment.

3.3 | Identification of Blood Lipid Derangements

LDL cholesterol was significantly associated with pancreas R2 water in both the unadjusted ($p = 0.031$) and adjusted ($p = 0.027$) models. HDL cholesterol was significantly associated with intra-hepatic fat in the unadjusted model only ($p = 0.040$), whereas triglycerides were significantly associated with intra-hepatic fat in both the unadjusted ($p = 0.021$) and adjusted ($p = 0.046$) models (Table 2). These non-linear relationships are depicted in Figure 2.

LDL dyslipidaemia was associated with intra-pancreatic fat in the unadjusted model only ($p = 0.026$) and with pancreas R2 water in both the unadjusted ($p = 0.046$) and adjusted ($p = 0.009$) models (Table 3, Figure 4). HDL dyslipidaemia was significantly associated with intra-hepatic fat in both the unadjusted ($p = 0.015$) and adjusted ($p = 0.047$) models, and with intra-pancreatic fat in both the unadjusted ($p = 0.009$) and adjusted ($p = 0.015$) models. HDL dyslipidaemia was also significantly associated with pancreas R2 water in the unadjusted model only ($p = 0.026$) (Table 3, Figure 4). Triglyceride dyslipidaemia was significantly associated with intra-hepatic fat in both the unadjusted ($p = 0.002$) and adjusted ($p = 0.046$) models. Additionally, it was associated with intra-pancreatic fat ($p = 0.031$), liver R2 water ($p = 0.051$), and pancreas R2 water ($p = 0.035$) in the unadjusted models only (Table 3, Figure 4).

In summary, LDL cholesterol was consistently associated with pancreas R2 water in both unadjusted and adjusted models, whereas HDL cholesterol was linked to intra-hepatic fat only in unadjusted analyses and triglycerides were associated with intra-hepatic fat in both models (with non-linear patterns). Across dyslipidaemia categories, LDL dyslipidaemia remained associated with pancreas R2 water after adjustment, whereas HDL and triglyceride dyslipidaemia showed the most consistent adjusted associations with intra-hepatic and/or intra-pancreatic fat, with several additional biomarker links present only before adjustment.

4 | Discussion

To the best of our knowledge, this was the first study to identify six common metabolic derangements with the use of four automated and standardised magnetic resonance signatures. ^{1}H-magnetic resonance spectroscopy, a technique that yields information on chemical components by separating the water

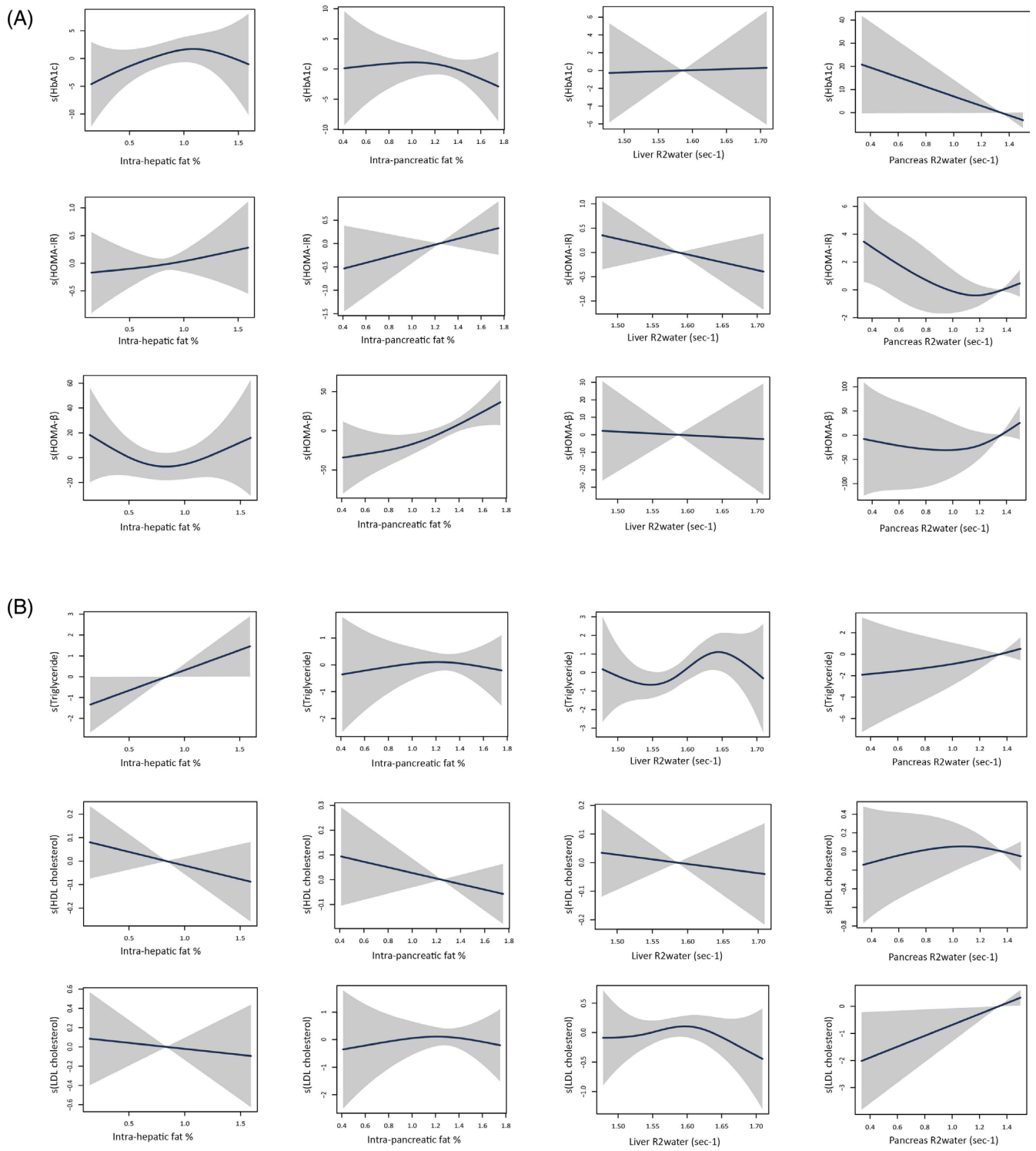

FIGURE 2 | Associations of (A) glucose metabolism and (B) lipid metabolism parameters with magnetic resonance signatures. Each y-axis displays partial residual plots of continuous magnetic resonce signatures. The grey shaded areas represent 95% confidence intervals from generalised additive models with P-spline smoothing, adjusted for age, sex and body mass index. Abbreviations: HbA1c, glycated haemoglobin; HOMA-β, Homeostasis model assessment of β-cell function; HOMA-IR, Homeostasis model assessment of insulin resistance; HDL, high-density lipoprotein cholesterol; LDL, low-density lipoprotein cholesterol.

resonance from confounding proton resonance (T2-correction), was employed for its high accuracy in quantifying tissue fat fraction and R2 of water [25, 26]. The standardised single breath-hold HISTO sequence at 3.0 Tesla used in the present study has considerable advantages over other imaging techniques, such as computed tomography and ultrasounds. These advantages include high speed, reproducibility, automated postprocessing–eliminating the potential for human error, and offline automation enabling the simultaneous provision of spectral images of voxel fat fraction and R2 of water with high speed [27]. The

TABLE 3 | Associations of the studied metabolic derangements with magnetic resonance signatures.

		Univariable logistic regression parameters					Multivariable logistic regression parameters				
Metabolic derangement	**Signature**	**Cut-off value**	**Estimate**	**SE**	***p***	**AUC**	**Cut-off value**	**Estimate**	**SE**	***p***	**AUC**
Prediabetes/ diabetes	Intra-hepatic fat	2.93	0.97	0.55	0.080	0.57	1.89	−2.09	1.14	0.068	0.66
	Intra-pancreatic fat	14.54	0.89	0.43	0.037*	0.60	45.52	−1.46	0.88	0.098	0.66
	Liver R2 water	40.09	−0.48	0.43	0.264	0.55	48.61	−15.77	818.51	0.985	0.65
	Pancreas R2 water	22.34	0.63	0.42	0.131	0.58	25.30	−1.48	0.67	0.055	0.69
Insulin resistance (higher HOMA-IR)	Intra-hepatic fat	6.36	1.03	0.43	0.017*	0.62	7.51	−1.58	1.45	0.991	0.77
	Intra-pancreatic fat	11.82	1.06	0.48	0.026*	0.61	11.82	0.95	0.53	0.073	0.73
	Liver R2 water	43.28	−0.80	0.59	0.179	0.55	43.28	−0.88	0.62	0.157	0.67
	Pancreas R2 water	22.64	1.11	0.44	0.012*	0.63	22.64	1.16	0.48	0.016*	0.67
Insulin deficiency (lower HOMA-β)	Intra-hepatic fat	6.74	1.29	0.44	0.003*	0.66	12.84	1.74	0.61	0.004*	0.72
	Intra-pancreatic fat	14.54	1.37	0.46	0.003*	0.65	14.54	2.04	0.60	0.001*	0.73
	Liver R2 water	37.96	1.03	0.43	0.017*	0.62	37.96	1.10	0.45	0.014*	0.70
	Pancreas R2 water	21.75	0.72	0.46	0.119	0.58	25.30	1.58	0.73	0.031*	0.70
Triglyceride dyslipidaemia	Intra-hepatic fat	7.13	1.36	0.44	0.002*	0.66	2.93	1.67	0.83	0.046*	0.75
	Intra-pancreatic fat	11.82	1.11	0.52	0.031*	0.60	8.56	1.16	0.70	0.098	0.74
	Liver R2 water	38.81	0.83	0.42	0.051	0.60	30.92	−16.10	592.22	0.978	0.72
	Pancreas R2 water	23.82	0.92	0.44	0.035*	0.61	20.26	1.11	0.82	0.175	0.72
HDL dyslipidaemia	Intra-hepatic fat	12.08	−1.15	0.47	0.015*	0.61	3.70	−1.32	0.66	0.047*	0.78
	Intra-pancreatic fat	11.82	−1.42	0.55	0.009*	0.63	9.10	−1.99	0.82	0.015*	0.80
	Liver R2 water	35.61	−0.62	0.48	0.198	0.56	41.58	0.84	0.56	0.134	0.77
	Pancreas R2 water	23.23	−0.96	0.43	0.026*	0.62	26.19	−1.21	0.87	0.162	0.77

(Continues)

TABLE 3 | (Continued)

Metabolic derangement	Signature	Univariable logistic regression parameters					Multivariable logistic regression parameters				
		Cut-off value	Estimate	SE	*p*	AUC	Cut-off value	Estimate	SE	*p*	AUC
LDL dyslipidaemia	Intra-hepatic fat	8.27	−0.31	0.46	0.496	0.54	5.98	−0.58	0.53	0.272	0.71
	Intra-pancreatic fat	4.75	−1.94	0.87	0.026*	0.57	4.75	−1.74	0.93	0.062	0.72
	Liver R2 water	42.22	−1.23	0.67	0.065	0.59	43.07	−1.17	0.81	0.146	0.71
	Pancreas R2 water	24.71	1.02	0.5	0.046*	0.59	25.90	2.08	0.80	0.009*	0.74

Note: Multivariable model was adjusted for age, sex and body mass index.
Abbreviations: AUC, Area under the curve; HDL, high-density lipoprotein cholesterol; HOMA-β, Homeostasis model assessment of β-cell function; HOMA-IR, Homeostasis model assessment of insulin resistance; LDL, low-density lipoprotein cholesterol; SE, standard error.
*Indicates $p < 0.05$.

observation that triglyceride dyslipidaemia was identifiable by intra-hepatic fat on imaging confirms the validity of our measurements, as this associaiton is physiologically expected [6, 28]. Although the link between ectopic fat (e.g., hepatic steatosis) and metabolic disorders is well established, our study extends this literature by using standardised, automated magnetic resoance signatures and by incorporating R2 water (a quantitative relaxometry measure) alongside fat fraction, enabling assessment of both lipid- and iron-related tissue characteristics. Importantly, prediabetes/diabetes was significantly associated with intra-pancreatic fat in the unadjusted model but this association was not observed after adjustment for age, sex and body mass index. This may reflect confounding by adiposity and related factors, as well as heterogeneity within the prediabetes/diabetes group (e.g., variation in disease duration, treatment and extent of glycaemic control). In addition, glycated haemoglobin is a composite marker of average glycaemia and may be less closely aligned with tissue-level compositional changes captured by magnetic resoance (i.e., fat fraction and R2 water), particularly in early or well-controlled disease. Taken together, these findings suggest that the magnetic resonance signatures investigated in the present study may be more sensitive to underlying insulin traits and dyslipidaemias than to a glycaemia-defined diagnosis in this cohort.

One of the key findings of the present study was that lower HOMA-β (as a binary variable) was statistically significantly associated with all four imaging signatures (intra-hepatic fat, intra-pancreatic fat liver R2 water, pancreas R2 water). Further, HOMA-β (as a continuous variable) had statistically significant associations with intra-pancreatic fat in the analyses adjusted for age, sex and body mass index. This finding highlights the importance of intra-pancreatic fat in diagnosing or predicting metabolic derangements, as postulated in the PANDORA hypothesis [4]. The hypothesis posits that increased intra-pancreatic fat is an early morphological change in the organ and a contributing factor to new-onset diabetes (among other diseases of the pancreas) [29]. These findings reinforce the notion that intra-pancreatic fat holds potential as a noninvasive biomarker of insulin deficiency, which could be the key to enabling the monitoring of the progression of diabetes and the progressive decline of pancreatic β cell mass [30]. Various morphological changes of pancreatic β cells lead to insulin deficiency (including β cell hypertrophy, hyperplasia and early β cell dedifferentiation), occurring during β cell compensation to increase β cell mass in response to hyperglycaemia [31, 32]. Therefore, even within a normal range of fasting plasma glucose, β cell function may begin to decline before a diagnosis of diabetes mellitus [30]. It is conceivable that intra-pancreatic fat as a magnetic resonance signature could be used in clinical practice in addition to the routinely used blood biomarkers to identify early morphological changes of β cells. Previous studies observed that increased intra-pancreatic fat deposition was associated with indices of pancreatic β cell dysfunction in health, obesity, glucose intolerance state, and non-alcoholic fatty liver disease [33–35]. Though insulin-producing β cells cannot be differentiated from non-insulin-producing pancreatic cells by means of imaging in vivo, animal studies have established that increase in intra-pancreatic fat deposition parallels the development of pancreatic β cell dysfunction [36]. In addition, evidence from randomised controlled trials showed that β cell function was restored by decreasing intra-pancreatic fat through energy restriction or exercise interventions [37, 38]. In contrast, some studies found no association between intra-pancreatic fat deposition and insulin deficiency [39–41]. The contradictory findings may be due to methodological differences in measuring intra-pancreatic fat and insulin deficiency and differences in ethnicity and age. Also, previous studies used linear analyses, possibly missing the non-linear relationship we found between intra-pancreatic fat and HOMA-β.

Another key finding was that LDL dyslipidaemia (as a binary variable) was significantly associated with pancreas R2 water. Further, the association between LDL cholesterol (as a continuous variable) and pancreas R2 water was statistically significant. The above findings, coupled with the significant association between insulin resistance and pancreas R2 water, underscore the important role of pancreas R2 water as a possible indicator for

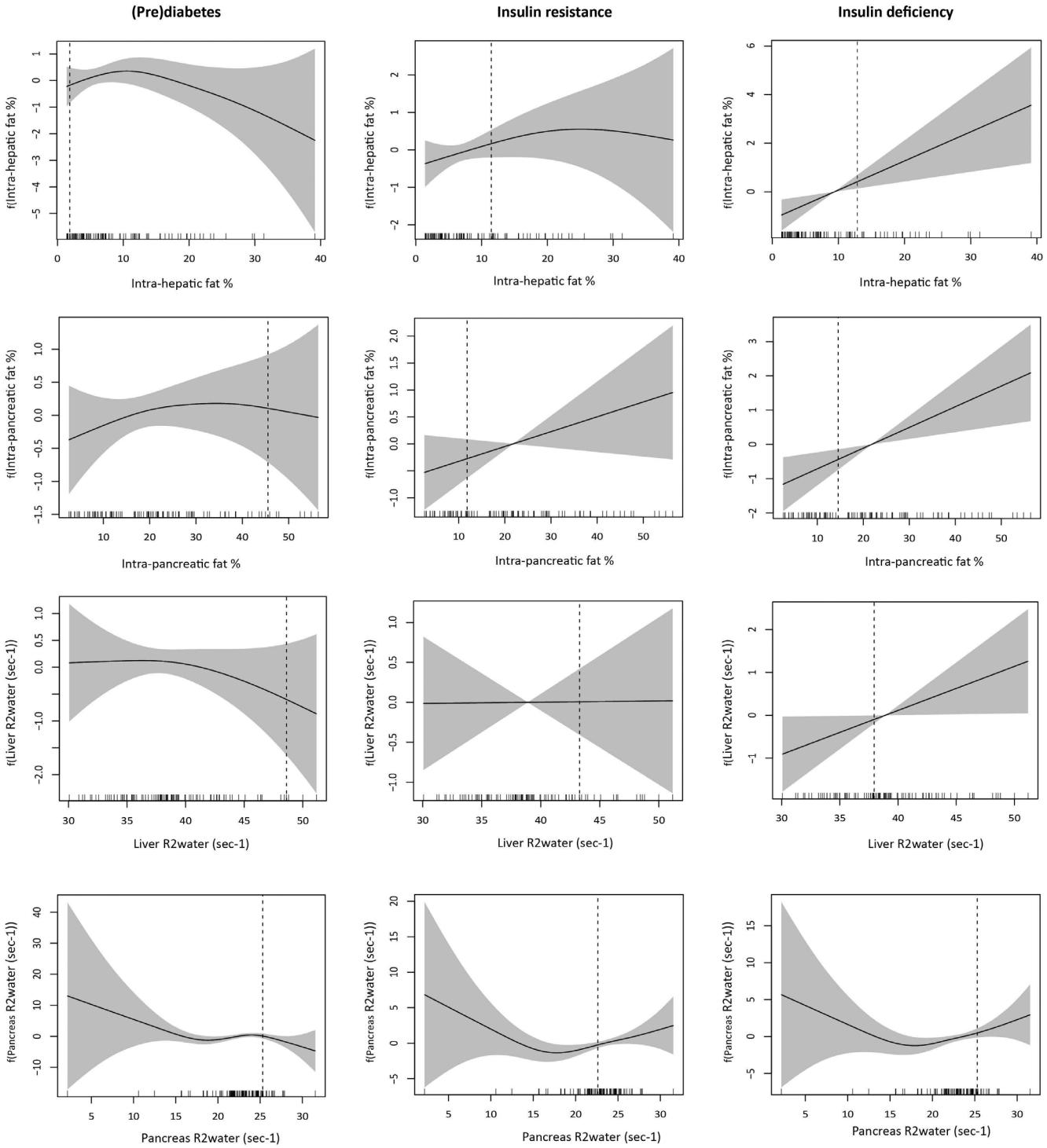

FIGURE 3 | Associations of glucose metabolism derangements with magnetic resonance signatures. Associations were modelled using logistic generalised additive models adjusted for age, sex and body mass index. The dotted line indicates the optimal cut-off value identified using CatPredi. Tick marks on the x-axis represent observed data points. The y-axis shows the partial effect of each variable, and shaded areas denote 95% confidence intervals.

glucose and lipid metabolism. Regulations of glucose and lipid metabolism are vital for maintaining health whereas dysregulation can lead to various disorders, including diabetes, fatty liver and atherosclerosis [3]. Elevated LDL cholesterol is a well-known risk factor for developing atherosclerotic cardiovascular disease [42]. LDL cholesterol is also the primary target for statins, which competitively inhibit 3-hydroxy-3-methylglutaryl coenzyme A (HMG-CoA) reductase—the enzyme that catalyses the rate-limiting step in cholesterol biosynthesis [43, 44]. The findings that LDL cholesterol was significantly associated with pancreas R2 water opens up an opportunity for assessing metabolic outcomes resulting from the interaction of iron and cholesterol metabolisms. Experimental model and clinical research studies have revealed links between the two metabolic

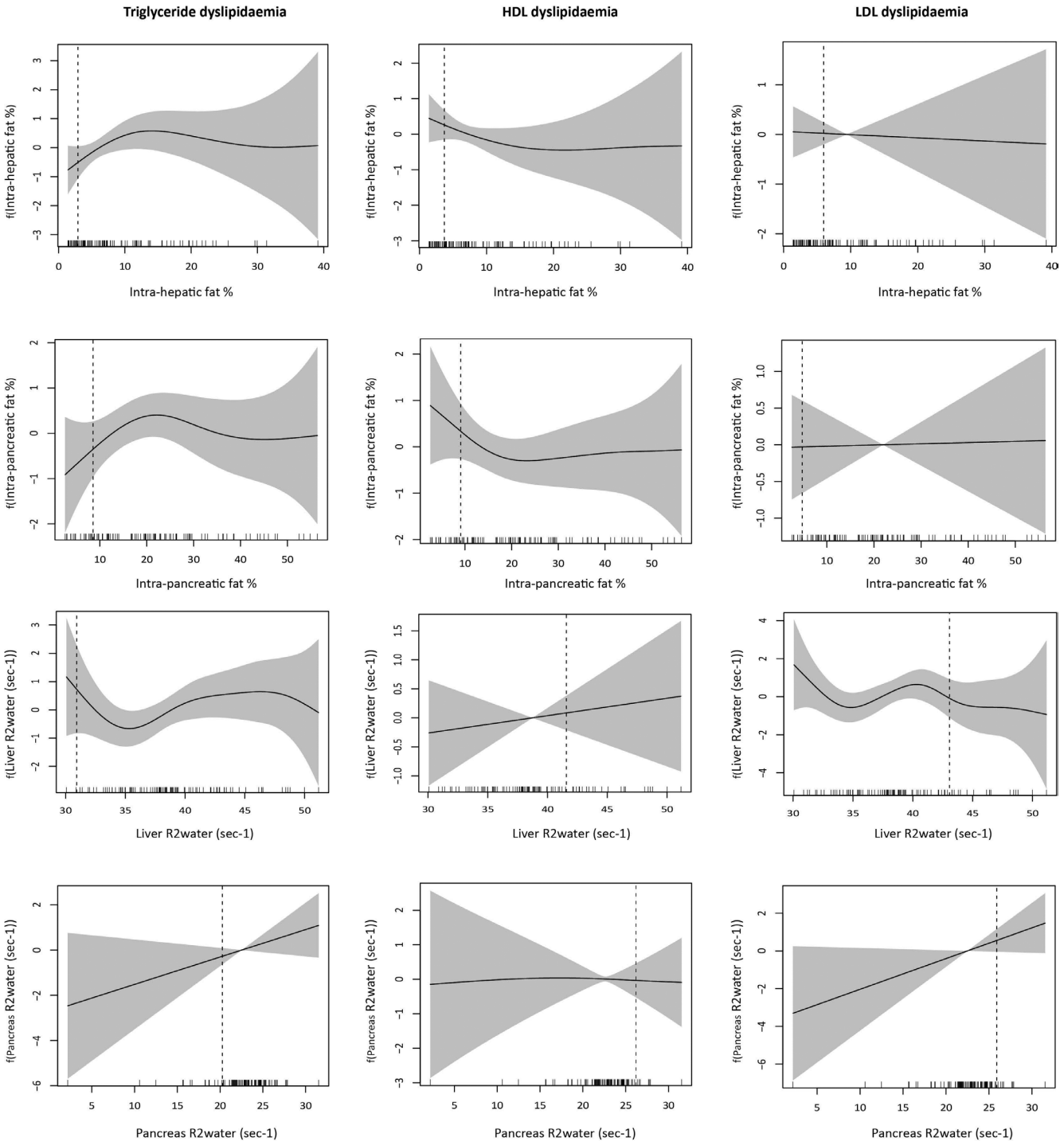

FIGURE 4 | Associations of lipid metabolism derangements with magnetic resonance signatures. Associations were modelled using logistic generalised additive models adjusted for age, sex and body mass index. The dotted line indicates the optimal cut-off value identified using CatPredi. Tick marks on the x-axis represent observed data points. The y-axis shows the partial effect of each variable, and shaded areas denote 95% confidence intervals.

pathways [45]. In addition, our 2023 study showed that pancreas R2 water was significantly associated with the iron-regulating hormone hepcidin [46]. Hepcidin is upregulated in response to increased body iron stores to prevent iron overload by inhibiting iron absorption from gut enterocytes, reducing iron recycling by macrophages, and promoting iron sequestration in hepatocytes [47]. Reduced levels of hepcidin lead to an over-expression of ferroportin (the transmembrane iron exporter in cells), resulting in iron deposition in the pancreas and other organs [48]. Changes in iron metabolism are associated with changes in cholesterol synthesis pathways [43]. Iron is an integral part of enzymes, transporters and transcription factors that control cholesterol biosynthesis involved in lipid metabolism and may exert a direct effect on the intra-pancreatic fat load [49]. There is evidence that elevated iron levels were correlated with increased mRNA expression of several genes involved in cholesterol biosynthesis

[49]. Furthermore, statins induce haem oxygenase-1 (the rate-limiting enzyme in haem catabolism) and suppress hepcidin expression by inhibiting HMG-CoA reductase [50]. Haem oxygenase-1 is key to the clearance of haemoglobin-derived iron by macrophages, reducing non-transferrin-bound iron and oxidative damage that adds to cardiovascular disease [50]. Given that the pancreas is relevant to both iron and cholesterol metabolism, further research is warranted to establish the mechanisms of these links and how pancreas R2 water may be used as a magnetic resonance signature of these interactions.

In addition to LDL dyslipidaemia, we also observed that HDL dyslipidaemia was significantly associated with intra-pancreatic fat in both unadjusted model and after taking into account body mass index, age and sex. This finding is biologically plausible as HDL particles are thought to preserve β-cell function and promote insulin sensitivity, and lower HDL cholesterol may therefore accompany (or contribute to) intra-pancreatic fat deposition and impaired glucose homeostasis [51–54]. However, given the cross-sectional design of the present study, the directionality of the association cannot be established and future studies should investigate whether HDL cholesterol (and HDL functionality) is independently linked to intra-pancreatic fat and subsequent changes in insulin traits [55].

Future research should prioritise external validation of the automated, standardised magnetic resonance signatures investigated in the present study across different vendors and populations. Prospective and longitudinal studies are also needed to determine whether pancreas and liver fat fraction and R2 water measurements can predict incident dyslipidaemia, progression to clinically meaningful endpoints (e.g., MASLD and cardiovascular events), and responses to lifestyle or pharmacological interventions, ideally compared directly with models based on routinely collected clinical variables and blood biomarkers. In parallel, future work should evaluate the incremental value and interpretability of combining magnetic resonance-derived organ-specific signatures with laboratory measures and medication data, including calibration, clinically relevant decision thresholds, and subgroup performance, to mitigate the risk of bias in real-world application. Finally, translational studies should assess workflow feasibility and health-economic implications, including whether opportunistic metabolic phenotyping from routine abdominal magnetic resonance imaging can be implemented cost-effectively, with appropriate reporting standards, governance and quality control.

The present study has several limitations. First, the study population consisted of individuals with a history of pancreatitis [29], potentially limiting generalisability to broader populations who do not have a history of pancreatitis. However, this enabled investigation of a relatively homogeneous, high-risk cohort long after hospital discharge. As a proof-of-principle investigation conducted in an at-risk cohort, the present study did not include a healthy control group. Accordingly, future studies should incorporate healthy controls and independent external validation in dedicated type 2 diabetes cohorts to confirm robustness and clinical usefulness of our findings. Second, although insulin traits were not verified using in vivo gold-standard methods such as a hyperglycaemic clamp or intravenous glucose tolerance test, HOMA-β served as a useful noninvasive tool for estimating β-cell function in the present study. Future research may need to explore the use of these gold-standard techniques to validate our findings. Third, the labelling of our participants as insulin-deficient and non-insulin-deficient may be suboptimal. For operational purposes, participants were dichotomised using cohort-specific median cut-offs. We acknowledge that, in a pancreatitis-only cohort without a control group, these median-based thresholds should not be interpreted as clinical definitions of insulin deficiency and are not directly comparable with proposed cut-offs in general populations. Fourth, insulin dosing and other glucose-lowering therapies, which provide important information on insulin deficiency and resistance, were not collected systematically in this proof-of-principle study. Future investigations should incorporate medication type, dose and duration to improve metabolic phenotyping and clinical interpretability [56]. Fifth, although LDL cholesterol was calculated rather than directly measured, this approach reflects standard laboratory practice [52, 54]. Nevertheless, calculated values may introduce some estimation error, which could affect the precision of associations with metabolic outcomes [57–59]. Future studies could include directly measured LDL cholesterol to further validate our findings. Sixth, histological data from the pancreas and liver quantifying intra-pancreatic and intra-hepatic fat were unavailable. In addition, the magnetic resonance signatures used in this study (fat fraction and R2 water) do not enable characterisation of hepatic inflammation (e.g., steatohepatitis). However, carrying out biopsies would be unethical and unnecessary in our study population. Moreover, biopsies also have several limitations, including sampling errors, inter-observer variability, and risk of complications due to their invasive nature. Seventh, using a single voxel to determine the imaging biomarkers in the whole pancreas might have introduced sampling error. However, an earlier study found that intra-pancreatic fat deposition did not differ in the head, body and tail of the organ [10]. Eighth, the relaxometry signal R2* of the pancreas could be viewed as a more representative biomarker of iron than the pancreas R2 water used in the present study. However, there is currently no standardised automated imaging protocol for pancreatic iron measurements, and T2 and T2* values of the pancreas have not been validated against biopsy for the quantification of iron in the pancreas [60]. Last, implementation of this magnetic resonance-based protocol at scale may be challenging in some healthcare settings because of cost or limited access to magnetic resonance examinations. However, though computed tomography is more widely available, it does not provide the same standardised quantitative signatures and involves ionising radiation.

In conclusion, while associations between ectopic fat and metabolic disorders have been reported previously, the novelty of the present work lies in moving beyond the general concept of 'fat–metabolic risk' by leveraging standardised, automated magnetic resonance quantitative signatures of both the pancreas and liver (fat fraction and R2 water). This approach enables the identification of multiple metabolic derangements using modelling strategies that accommodate non-linear relationships. Together, these findings support the use of standardised magnetic resonance signatures of the pancreas and liver as complementary markers of metabolic dysfunction, offering a scalable and reproducible framework for metabolic risk phenotyping in at-risk populations.

Author Contributions

W.K. and J.K. contributed to participant recruitment and data acquisition. W.K. conducted all data analyses and interpretation and wrote the manuscript. J.K., L.S.-H., X.S., Y.L. and M.S.P. contributed to the critical revision of the manuscript. M.S.P. conceptualised and supervised the study.

Acknowledgements

This study was part of the COSMOS programme. Open access publishing facilitated by The University of Auckland, as part of the Wiley - The University of Auckland agreement via the Council of Australasian University Librarians

Funding

The authors have nothing to report.

Conflicts of Interest

The authors declare no conflicts of interest.

Data Availability Statement

The data that support the findings of this study are available from the corresponding author upon reasonable request.

References

1. A. Pirillo, M. Casula, E. Olmastroni, G. D. Norata, and A. L. Catapano, "Global Epidemiology of Dyslipidaemias," *Nature Reviews Cardiology* 18, no. 10 (2021): 689–700, https://doi.org/10.1038/s41569-021-00541-4.

2. G. Danaei, M. M. Finucane, Y. Lu, et al., "National, Regional, and Global Trends in Fasting Plasma Glucose and Diabetes Prevalence Since 1980: Systematic Analysis of Health Examination Surveys and Epidemiological Studies With 370 Country-Years and 2·7 Million Participants," *Lancet* 378, no. 9785 (2011): 31–40, https://doi.org/10.1016/S0140-6736(11)60679-X.

3. L. Chen, X. Chen, X. Huang, B. Song, Y. Wang, and Y. Wang, "Regulation of Glucose and Lipid Metabolism in Health and Disease," *Science China. Life Sciences* 62, no. 11 (2019): 1420–1458, https://doi.org/10.1007/s11427-019-1563-3.

4. M. S. Petrov, "Fatty Change of the Pancreas: The Pandora's Box of Pancreatology," *Lancet Gastroenterology and Hepatology* 8, no. 7 (2023): 671–682, https://doi.org/10.1016/S2468-1253(23)00064-X.

5. M. S. Petrov and R. Taylor, "Intra-Pancreatic Fat Deposition: Bringing Hidden Fat to the Fore," *Nature Reviews. Gastroenterology and Hepatology* 19, no. 3 (2022): 153–168, https://doi.org/10.1038/s41575-021-00551-0.

6. J. Ko, I. R. Sequeira, L. Skudder-Hill, J. Cho, S. D. Poppitt, and M. S. Petrov, "Metabolic Traits Affecting the Relationship Between Liver Fat and Intrapancreatic Fat: A Mediation Analysis," *Diabetologia* 66, no. 1 (2023): 190–200, https://doi.org/10.1007/s00125-022-05793-4.

7. L. Skudder-Hill, I. R. Sequeira-Bisson, J. Ko, S. D. Poppitt, and M. S. Petrov, "The Moderating Effect of Cardiometabolic Factors on the Association Between Hepatic and Intrapancreatic Fat," *Obesity* 32, no. 12 (2024): 2310–2320, https://doi.org/10.1002/oby.24154.

8. M. F. Xia, H. Bian, and X. Gao, "NAFLD and Diabetes: Two Sides of the Same Coin? Rationale for Gene-Based Personalized NAFLD Treatment," *Frontiers in Pharmacology* 10 (2019): 10, https://doi.org/10.3389/fphar.2019.00877.

9. L. A. Adams, J. F. Lymp, J. St Sauver, et al., "The Natural History of Nonalcoholic Fatty Liver Disease: A Population-Based Cohort Study," *Gastroenterology* 129, no. 1 (2005): 113–121, https://doi.org/10.1053/j.gastro.2005.04.014.

10. L. Skudder-Hill, I. R. Sequeira, J. Cho, J. Ko, S. D. Poppitt, and M. S. Petrov, "Fat Distribution Within the Pancreas According to Diabetes Status and Insulin Traits," *Diabetes* 71, no. 6 (2022): 1182–1192, https://doi.org/10.2337/db21-0976.

11. R. G. Singh, H. D. Yoon, S. D. Poppitt, L. D. Plank, and M. S. Petrov, "Ectopic Fat Accumulation in the Pancreas and Its Biomarkers: A Systematic Review and Meta-Analysis," *Diabetes/Metabolism Research and Reviews* 33, no. 8 (2017): e2918, https://doi.org/10.1002/dmrr.2918.

12. P. Dongiovanni, A. L. Fracanzani, S. Fargion, and L. Valenti, "Iron in Fatty Liver and in the Metabolic Syndrome: A Promising Therapeutic Target," *Journal of Hepatology* 55, no. 4 (2011): 920–932, https://doi.org/10.1016/j.jhep.2011.05.008.

13. W. Kimita and M. S. Petrov, "Iron Metabolism and the Exocrine Pancreas," *Clinica Chimica Acta* 511 (2020): 167–176, https://doi.org/10.1016/j.cca.2020.10.013.

14. J. Virostko, "Quantitative Magnetic Resonance Imaging of the Pancreas of Individuals With Diabetes," *Front Endocrinol (Lausanne)* 11 (2020): 592349, https://doi.org/10.3389/fendo.2020.592349.

15. B. M. Abunahel, B. Pontre, H. Kumar, and M. S. Petrov, "Pancreas Image Mining: A Systematic Review of Radiomics," *European Radiology* 31, no. 5 (2021): 3447–3467, https://doi.org/10.1007/s00330-020-07376-6.

16. B. M. Abunahel, B. Pontre, and M. S. Petrov, "Effect of Gray Value Discretization and Image Filtration on Texture Features of the Pancreas Derived From Magnetic Resonance Imaging at 3T," *Journal of Imaging* 8, no. 8 (2022): 220, https://doi.org/10.3390/jimaging8080220.

17. B. M. Abunahel, B. Pontre, J. Ko, and M. S. Petrov, "Towards Developing a Robust Radiomics Signature in Diffuse Diseases of the Pancreas: Accuracy and Stability of Features Derived From T1-Weighted Magnetic Resonance Imaging," *Journal of Medical Imaging and Radiation Sciences* 53, no. 3 (2022): 420–428, https://doi.org/10.1016/j.jmir.2022.04.002.

18. H. Kumar, S. V. DeSouza, and M. S. Petrov, "Automated Pancreas Segmentation From Computed Tomography and Magnetic Resonance Images: A Systematic Review," *Computer Methods and Programs in Biomedicine* 178 (2019): 319–328, https://doi.org/10.1016/j.cmpb.2019.07.002.

19. A. Lin, O. Andronesi, W. Bogner, et al., "Minimum Reporting Standards for In Vivo Magnetic Resonance Spectroscopy (MRSinMRS): Experts' Consensus Recommendations," *NMR in Biomedicine* 34, no. 5 (2021): e4484, https://doi.org/10.1002/nbm.4484.

20. M. Sampson, C. Ling, Q. Sun, et al., "A New Equation for Calculation of Low-Density Lipoprotein Cholesterol in Patients With Normolipidemia and/or Hypertriglyceridemia," *JAMA Cardiology* 5, no. 5 (2020): 540–548, https://doi.org/10.1001/jamacardio.2020.0013.

21. C. E. Stuart, R. G. Singh, G. C. Alarcon Ramos, et al., "Relationship of Pancreas Volume to Tobacco Smoking and Alcohol Consumption Following Pancreatitis," *Pancreatology* 20, no. 1 (2020): 60–67, https://doi.org/10.1016/j.pan.2019.10.009.

22. American Diabetes Association Professional Practice Committee, "2. Diagnosis and Classification of Diabetes: Standards of Care in Diabetes-2025," *Diabetes Care* 48, no. 1 Suppl 1 (2025): S27–S49, https://doi.org/10.2337/dc25-S002.

23. Expert Panel on Detection, Evaluation, and Treatment of High Blood Cholesterol in Adults, "Executive Summary of the Third Report of the National Cholesterol Education Program (NCEP) Expert Panel on Detection, Evaluation, and Treatment of High Blood Cholesterol in Adults (Adult Treatment Panel III)," *JAMA* 285, no. 19 (2001): 2486–2497, https://doi.org/10.1001/jama.285.19.2486.

24. I. Barrio, I. Arostegui, M. X. Rodríguez-Álvarez, and J. M. Quintana, "A New Approach to Categorising Continuous Variables in Prediction

Models: Proposal and Validation," *Statistical Methods in Medical Research* 26, no. 6 (2017): 2586–2602, https://doi.org/10.1177/0962280215601873.

25. S. B. Reeder, H. H. Hu, and C. B. Sirlin, "Proton Density Fat-Fraction: A Standardized MR-Based Biomarker of Tissue Fat Concentration," *Journal of Magnetic Resonance Imaging* 36, no. 5 (2012): 1011–1014, https://doi.org/10.1002/jmri.23741.

26. P. Sharma, D. R. Martin, N. Pineda, et al., "Quantitative Analysis of T2-Correction in Single-Voxel Magnetic Resonance Spectroscopy of Hepatic Lipid Fraction," *Journal of Magnetic Resonance Imaging* 29, no. 3 (2009): 629–635, https://doi.org/10.1002/jmri.21682.

27. P. Sharma and D. Martin, "An Efficient Workflow for Quantifying Hepatic Lipid and Iron Deposition Using LiverLab," *MAGNETOM Flash* 3, no. 58 (2014): 12–17.

28. L. Skudder-Hill, I. R. Sequeira-Bisson, J. Ko, S. Poppitt, and M. S. Petrov, "Relationship of Fat Deposition in the Liver and Pancreas With Cholecystectomy," *Obesity Facts* 18, no. 5 (2025): 468–480, https://doi.org/10.1159/000545781.

29. J. Ko and M. S. Petrov, "Intra-Pancreatic Fat Deposition and Pancreatitis: Insights From the COSMOS Program," *Diabetes, Metabolic Syndrome and Obesity* 18 (2025): 1489–1500, https://doi.org/10.2147/DMSO.S400276.

30. Y. Saisho, A. E. Butler, J. J. Meier, et al., "Pancreas Volumes in Humans From Birth to Age One Hundred Taking Into Account Sex, Obesity, and Presence of Type-2 Diabetes," *Clinical Anatomy* 20, no. 8 (2007): 933–942, https://doi.org/10.1002/ca.20543.

31. M. E. Cerf, "Beta Cell Dysfunction and Insulin Resistance," *Frontiers in Endocrinology* 4 (2013): 37, https://doi.org/10.3389/fendo.2013.00037.

32. T. Mezza, G. Muscogiuri, G. P. Sorice, et al., "Insulin Resistance Alters Islet Morphology in Nondiabetic Humans," *Diabetes* 63, no. 3 (2014): 994–1007, https://doi.org/10.2337/db13-1013.

33. I. Lingvay, V. Esser, J. Legendre, et al., "Noninvasive Quantification of Pancreatic Fat in Humans," *Journal of Clinical Endocrinology and Metabolism* 94, no. 10 (2009): 4070–4076, https://doi.org/10.1210/jc.2009-0584.

34. M. Heni, J. Machann, H. Staiger, et al., "Pancreatic Fat Is Negatively Associated With Insulin Secretion in Individuals With Impaired Fasting Glucose and/or Impaired Glucose Tolerance: A Nuclear Magnetic Resonance Study," *Diabetes, Metabolic Syndrome and Obesity: Targets and Therapy* 26, no. 3 (2010): 200–205, https://doi.org/10.1002/dmrr.1073.

35. C. Chiyanika, D. F. Chan, S. C. Hui, et al., "The Relationship Between Pancreas Steatosis and the Risk of Metabolic Syndrome and Insulin Resistance in Chinese Adolescents With Concurrent Obesity and Non-Alcoholic Fatty Liver Disease," *Pediatric Obesity* 15, no. 9 (2020): e12653, https://doi.org/10.1111/ijpo.12653.

36. Y. Wen, C. Chen, X. Kong, et al., "Pancreatic Fat Infiltration, β-Cell Function and Insulin Resistance: A Study of the Young Patients With Obesity," *Diabetes Research and Clinical Practice* 187 (2022): 109860, https://doi.org/10.1016/j.diabres.2022.109860.

37. E. L. Lim, K. G. Hollingsworth, B. S. Aribisala, M. J. Chen, J. C. Mathers, and R. Taylor, "Reversal of Type 2 Diabetes: Normalisation of Beta Cell Function in Association With Decreased Pancreas and Liver Triacylglycerol," *Diabetologia* 54, no. 10 (2011): 2506–2514, https://doi.org/10.1007/s00125-011-2204-7.

38. M. Li, Q. Zheng, J. D. Miller, et al., "Aerobic Training Reduces Pancreatic Fat Content and Improves β-Cell Function: A Randomized Controlled Trial Using IDEAL-IQ Magnetic Resonance Imaging," *Diabetes/Metabolism Research and Reviews* 38, no. 4 (2022): e3516, https://doi.org/10.1002/dmrr.3516.

39. V. W. Wong, G. L. Wong, D. K. Yeung, et al., "Fatty Pancreas, Insulin Resistance, and β-Cell Function: A Population Study Using Fat-Water Magnetic Resonance Imaging," *American Journal of Gastroenterology* 109, no. 4 (2014): 589–597, https://doi.org/10.1038/ajg.2014.1.

40. N. van der Zijl, G. Goossens, C. Moors, et al., "Ectopic Fat Storage in the Pancreas, Liver, and Abdominal Fat Depots: Impact on β-Cell Function in Individuals With Impaired Glucose Metabolism," *Journal of Clinical Endocrinology and Metabolism* 96, no. 2 (2011): 459–467, https://doi.org/10.1210/jc.2010-1722.

41. P. Begovatz, C. Koliaki, K. Weber, et al., "Pancreatic Adipose Tissue Infiltration, Parenchymal Steatosis and Beta Cell Function in Humans," *Diabetologia* 58, no. 7 (2015): 1646–1655, https://doi.org/10.1007/s00125-015-3544-5.

42. C. K. Lee, C. W. Liao, S. W. Meng, W. K. Wu, J. Y. Chiang, and M. S. Wu, "Lipids and Lipoproteins in Health and Disease: Focus on Targeting Atherosclerosis," *Biomedicine* 9, no. 8 (2021): 985, https://doi.org/10.3390/biomedicines9080985.

43. Cholesterol Treatment Trialists' (CTT) Collaborators, "The Effects of Lowering LDL Cholesterol With Statin Therapy in People at Low Risk of Vascular Disease: Meta-Analysis of Individual Data From 27 Randomised Trials," *Lancet (London, England)* 380, no. 9841 (2012): 581–590, https://doi.org/10.1016/S0140-6736(12)60367-5.

44. D. Maron, S. Fazio, and M. Linton, "Current Perspectives on Statins," *Circulation* 101, no. 2 (2000): 207–213, https://doi.org/10.1161/01.CIR.101.2.207.

45. S. Rockfield, R. Chhabra, M. Robertson, N. Rehman, R. Bisht, and M. Nanjundan, "Links Between Iron and Lipids: Implications in Some Major Human Diseases," *Pharmaceuticals (Basel, Switzerland)* 11, no. 4 (2018): 113, https://doi.org/10.3390/ph11040113.

46. W. Kimita, J. Ko, and M. S. Petrov, "Relationship of Iron Intake, Ferritin, and Hepcidin With the Transverse Relaxation Rate of Water Protons in the Pancreas," *Nutrients* 15, no. 17 (2023): 3727, https://doi.org/10.3390/nu15173727.

47. T. Ganz and E. Nemeth, "Hepcidin and Iron Homeostasis," *Biochimica et Biophysica Acta, Molecular Cell Research* 1823, no. 9 (2012): 1434–1443, https://doi.org/10.1016/j.bbamcr.2012.01.014.

48. D. M. Ward and J. Kaplan, "Ferroportin-Mediated Iron Transport: Expression and Regulation," *Biochimica et Biophysica Acta, Molecular Cell Research* 1823, no. 9 (2012): 1426–1433, https://doi.org/10.1016/j.bbamcr.2012.03.004.

49. R. M. Graham, A. C. G. Chua, K. W. Carter, et al., "Hepatic Iron Loading in Mice Increases Cholesterol Biosynthesis," *Hepatology* 52, no. 2 (2010): 462–471, https://doi.org/10.1002/hep.23712.

50. L. Mascitelli and M. R. Goldstein, "Might the Beneficial Effects of Statin Drugs Be Related to Their Action on Iron Metabolism?," *QJM* 105, no. 12 (2012): 1225–1229, https://doi.org/10.1093/qjmed/hcs204.

51. Y. Liu, J. Ko, L. Skudder-Hill, X. Shamaitijiang, I. R. Sequeira-Bisson, and M. S. Petrov, "Interplay Between Intra-Pancreatic Fat Deposition, Exchangeable Apolipoproteins, and Lipoprotein Subclasses," *Nutrition, Metabolism, and Cardiovascular Diseases* 36, no. 1 (2026): 104280, https://doi.org/10.1016/j.numecd.2025.104280.

52. L. Skudder-Hill, S. Coffey, I. R. Sequeira-Bisson, J. Ko, S. D. Poppitt, and M. S. Petrov, "Comprehensive Analysis of Dyslipidemia States Associated With Fat in the Pancreas," *Diabetes and Metabolic Syndrome: Clinical Research and Reviews* 17, no. 11 (2023): 102881, https://doi.org/10.1016/j.dsx.2023.102881.

53. Y. Liu, X. Shamaitijiang, L. Skudder-Hill, W. Kimita, I. R. Sequeira-Bisson, and M. S. Petrov, "Relationship of High-Density Lipoprotein Subfractions and Apolipoprotein A-I With Fat in the Pancreas," *Diabetes, Obesity and Metabolism* 27, no. 1 (2025): 123–133, https://doi.org/10.1111/dom.15990.

54. L. Skudder-Hill, I. R. Sequeira-Bisson, J. Ko, J. Cho, S. D. Poppitt, and M. S. Petrov, "Remnant Cholesterol, but Not Low-Density Lipoprotein Cholesterol, Is Associated With Intra-Pancreatic Fat Deposition,"

Diabetes, Obesity and Metabolism 25, no. 11 (2023): 3337–3346, https://doi.org/10.1111/dom.15233.

55. C. B. Leybourne, Y. Liu, and M. S. Petrov, "Excessive Intrapancreatic Fat Deposition and Risk of Pancreatic Diseases: Longitudinal Lohort Evidence From a Systematic Review With Population-Attributable Fraction Analysis," *American Journal of Gastroenterology* (2025), https://doi.org/10.14309/ajg.0000000000003799.

56. H. C. Agon, Y. Shen, and M. S. Petrov, "Effects of Glucose-Lowering Medications on Intrapancreatic Fat Deposition: A Systematic Review and Meta-Analysis of Randomized Controlled Trials," *Obesity Reviews* 27 (2026): e70087, https://doi.org/10.1111/obr.70087.

57. Y. Liu, I. R. Sequeira-Bisson, J. Ko, X. Shamaitijiang, L. Skudder-Hill, and M. S. Petrov, "Relationship of Intra-Pancreatic Fat Deposition With Low-Density Lipoprotein Subfractions and Hepatic Lipase," *Diabetes, Obesity and Metabolism* 27, no. 11 (2025): 6674–6681.

58. Y. Liu, L. Skudder-Hill, W. Kimita, X. Shamaitijiang, I. R. Sequeira-Bisson, and M. S. Petrov, "Associations of Intra-Pancreatic Fat Deposition With Triglyceride-Rich Lipoproteins and Lipoprotein Lipase," *Diabetes, Obesity and Metabolism* 27, no. 6 (2025): 3233–3241, https://doi.org/10.1111/dom.16338.

59. Y. Liu, L. Skudder-Hill, J. Ko, X. Shamaitijiang, I. R. Sequeira-Bisson, and M. S. Petrov, "Dysapolipoproteinaemia Influences the Relationship Between Very Low-Density Lipoprotein Cholesterol and Intra-Pancreatic Fat Deposition in Humans," *Nutrients* 17, no. 23 (2025): 3718, https://doi.org/10.3390/nu17233718.

60. A. Meloni, V. Positano, L. Pistoia, and F. Cademartiri, "Pancreatic Iron Quantification With MR Imaging: A Practical Guide," *Abdominal Radiology* 47, no. 7 (2022): 2397–2407, https://doi.org/10.1007/s00261-022-03552-y.